

A Large Gene Cluster in *Burkholderia xenovorans* Encoding Abietane Diterpenoid Catabolism^{∇†}

Daryl J. Smith,¹ Joonhong Park,² James M. Tiedje,³ and William W. Mohn^{1*}

Department of Microbiology and Immunology, Life Sciences Institute, University of British Columbia, Vancouver, British Columbia, Canada¹; School of Civil and Environmental Engineering, Yonsei University, Seoul, Republic of Korea²; and Center for Microbial Ecology, Michigan State University, East Lansing, Michigan³

Received 2 February 2007/Accepted 14 June 2007

Abietane diterpenoids are defense compounds synthesized by trees that are abundant in natural environments and occur as significant pollutants from pulp and paper production. *Burkholderia xenovorans* LB400 has diverse catabolic capabilities and represents an important group of heterotrophic bacteria in soil environments. The genome sequence of LB400 revealed homologs of the *dit* genes of *Pseudomonas abietaniphila* BKME-9, which encode abietane diterpenoid degradation. LB400 grew on abietic acid (AbA), dehydroabietic acid (DhA), palustric acid (PaA), and 7-oxo-DhA. A Xeotron microarray set, with probes for 8450 of the estimated 9000 LB400 genes, was used to compare the transcriptomes of LB400 growing on DhA versus on succinate. On DhA, 97 genes were upregulated, 43 of which were within an 80-kb cluster located on the 1.47-Mbp megaplasmid of LB400. Upregulated genes in this cluster encode a permease, a ring-hydroxylating dioxygenase system (DitA), a ring-cleavage dioxygenase (DitC), a P450 monooxygenase (DitQ), and enzymes catalyzing beta-oxidation-type reactions. Disruption of the *ditA1* gene, encoding the alpha-subunit of DitA, abolished growth on these abietanes. Analyses of the metabolism of abietanes by cell suspensions of wild-type LB400 and the *ditA1* mutant indicate a convergent pathway, with 7-oxo-DhA as a common intermediate for ring hydroxylation by DitA. Also, 7-oxo-PaA was identified as a metabolite of both AbA and PaA. Sequence analysis indicates that genes encoding this pathway have been horizontally transferred among *Betaproteobacteria* and *Gammaproteobacteria*.

Bacteria of the genus *Burkholderia* have been isolated from diverse environments and have significant interactions with both plants and animals. Some *Burkholderia* spp. are human pathogens, including *Burkholderia cepacia* (8), *B. pseudomallei* (38), and *B. mallei* (30). In plants, the relationship can be beneficial, preventing disease or promoting growth, nodule formation, or nitrogen fixation (7). Alternately, the relationship can be deleterious, causing disease (28). However, the niches of the majority of *Burkholderia* species likely are in plant rhizospheres where they involve nonpathogenic interactions (8). Catabolic diversity is an expected characteristic of *Burkholderia* species, permitting them to exploit the vast range of compounds synthesized by plants.

B. xenovorans LB400 was isolated from a PCB-contaminated landfill in New York State (16). The genome of LB400 was recently sequenced and annotated (5). This large bacterial genome is 9.7 Mbp and is comprised of three replicons, chromosome 1 (4.87 Mbp), chromosome 2 (3.36 Mbp), and a megaplasmid (1.47 Mbp), containing ~9,000 predicted genes. Much of the work on LB400 prior to genome sequencing focused on its metabolism of biphenyl and polychlorinated biphenyls; however, sequencing of the genome has revealed several other metabolic capabilities.

Studies of LB400 in a genomic context have included those focusing on biphenyl, as well as on the benzoate and C1 metabolic pathways (11–13). An additional catabolic capacity of LB400 was suggested when we previously identified 22 clustered genes in LB400 that are homologous to genes in the *dit* cluster of *Pseudomonas abietaniphila* BKME-9 (33), which encode abietane diterpenoid catabolism (20, 21, 33).

Catabolism of abietane diterpenoids is an environmentally significant process. Abietane diterpenoids are tricyclic, C-20, carboxylic acid-containing compounds produced by plants (see Fig. 4 for representative chemical structures). These compounds are a key component of the defense systems of coniferous trees (4). As such, abietane diterpenoids are synthesized in large quantities, which must be turned over within the carbon cycle of forest environments. Also, accumulation of diterpenoids during pulp and paper manufacturing is the major contributor to the toxicity of effluents from this industry (1, 17). Research on the microbial removal of these compounds by wastewater treatment systems has been the driving force behind investigations of their biodegradation. Studies of abietane diterpenoid catabolism by BKME-9 led to a proposed convergent dioxygenolytic pathway, involving a cytochrome P450 monooxygenase, a ring hydroxylating dioxygenase, and a ring cleavage dioxygenase. A range of bacteria, including members of the genus *Burkholderia*, were previously found to mineralize abietane diterpenoids (24). However, LB400 is the first such bacterium for which a complete genomic sequence is available, permitting genomic investigation of abietane diterpenoid catabolism.

We describe here for the first time the growth of LB400 on four abietane diterpenoids. Using microarray transcriptomic

* Corresponding author. Mailing address: Department of Microbiology and Immunology, Life Sciences Institute, The University of British Columbia, 2350 Health Sciences Mall, Vancouver, BC V6T 1Z3, Canada. Phone: (604) 822-4285. Fax: (604) 822-6041. E-mail: wmohn@interchange.ubc.ca.

† Supplemental material for this article may be found at <http://jb.asm.org/>.

∇ Published ahead of print on 22 June 2007.

TABLE 1. Strains and plasmids used in this study

Strain or plasmid	Genotype or description ^a	Source or reference
Strains		
<i>Burkholderia xenovorans</i>		
LB400	Wild type; grows on abietane diterpenoids	16
DitA1KO	<i>ditA1::accC1</i> ; Gm ^r	This study
<i>Escherichia coli</i> DH5 α		
S17-1	<i>endA1 hsdR17</i> ($r_K^- m_K^-$) <i>supE44 thi-1 recA1 gyrA</i> (Nal ^r) <i>relA1</i> Δ (<i>lacIZYA-argF</i>) <i>U169 deoR</i> [ϕ 80 <i>dlac</i> Δ (<i>lacZ</i>)M15] <i>recA pro thi hsdR</i> with integrated RP4-2-TcMu::Kna::Tn7; Tra ⁺ Tp ^r Sm ^r	Gibco-BRL 32
Plasmids		
pEX100T	<i>sacB</i> conjugable plasmid for gene replacement; Ap ^r	31
pX1918G	<i>xylE-accC1</i> fusion cassette-containing plasmid; Ap ^r Gm ^r	31
pDS2	1.8-kbp PCR amplicon containing LB400 <i>ditA1</i> cloned into the unique XmaI site of pEX100T	This study
pDS3	1,482-bp EcoRV-SmaI of pDS1 cloned into the SmaI site of pEX100T	This study

^a Gm^r, gentamicin resistance; Nal^r, nalidixic acid resistance; Ap^r, ampicillin resistance; Tp^r, trimethoprim resistance; Sm^r, streptomycin resistance.

analysis, we provide evidence that a single large cluster of LB400 *dit* genes encodes catabolism of DhA, the most abundant abietane, and associate a number of previously unrecognized genes with DhA catabolism. By knockout analysis, we tested the essentiality of *ditA1*, encoding a ring-hydroxylating dioxygenase, for abietane catabolism. With cell suspension assays, we compare metabolism of abietane diterpenoids by LB400 and BKME-9 and present evidence for novel routes for AbA and PaA degradation.

MATERIALS AND METHODS

Bacterial strains, plasmids, and culture conditions. The bacterial strains and plasmids used in the present study are listed in Table 1. *Escherichia coli* was cultured on Luria-Bertani (LB) medium and incubated at 37°C. *B. xenovorans* strains were cultured at 30°C. Frozen stocks of *B. xenovorans* strains were revived by streaking on 1.5% agar K1 plates, which were incubated for 3 to 4 days upside down with biphenyl crystals on the petri dish lid. Liquid *B. xenovorans* cultures were in LB without NaCl or in K1 mineral medium (12) supplemented with 1 g per liter succinate, 90 mg of abietic acid (AbA), 90 mg of dehydroabietic acid (DhA), 90 mg of palustric acid (PaA), or 95 mg of 7-oxo-DhA per liter. All liquid cultures were incubated on a rotary shaker at 200 to 250 rpm. The medium for strain DitA1KO also contained 10 mg of gentamicin/ml.

Cell suspension assays. LB400 and DitA1KO were cultured on succinate to mid-log phase (optical density at 600 nm [OD₆₀₀] = 0.4 to 0.6) and transferred three times, sequentially. The third transfers contained 1 liter of medium and were harvested by centrifugation for 10 min at 8,800 \times g, washed with K1 salts containing neither vitamins nor Hunter mix, and suspended at an OD₆₀₀ of ~3.0 in K1 medium. Each culture was then divided into four aliquots of ~50 ml that were amended with 300 μ M AbA, DhA, PaA, or 7-oxo-DhA. Control cell suspensions were prepared and incubated as described above; however, the cells were boiled for approximately 15 min prior to the addition of the abietane diterpenoids. Samples of 1.5 ml were collected at various time points, acidified with 2 to 3 drops of 1 M HCl, and frozen at -20°C for later analysis by gas chromatography-mass spectrometry (GC-MS).

After the samples were thawed, an internal standard of 12,14-dichlorodehydroabietic acid was added to each to a final concentration of 50 μ M, the samples were extracted twice with equal volumes of ethyl acetate, and pooled extracts were dried over anhydrous Na₂SO₄. Analytes were derivatized by using diazomethane. GC electron impact MS of methyl ester derivatives was conducted as previously described (33), using an Agilent Technologies 6890N Network GC system equipped with an Agilent 5973 mass selective detector. National Institute of Standards and Technology MS Search (2.0) was used to analyze mass spectral data.

Transcriptome cultures. For analysis of succinate-grown cells, LB400 was cultured on succinate to mid-log phase and transferred three times, sequentially. The third transfers were in duplicate and contained 200 ml of medium. After

approximately 18 h of incubation, cultures reached mid-log phase (OD₆₀₀ of 0.5), and the cells were harvested as described below.

For analysis of DhA-grown cells, LB400 from a second serial culture on succinate (as described above) was transferred to medium with DhA, at an initial OD₆₀₀ of 0.01. After approximately 140 h of incubation, the culture had reached late log phase (OD₆₀₀ of 0.15), and cells were transferred to fresh DhA medium at an initial OD of 0.001. After approximately 48 h of incubation, the culture had reached a mid- to late-log phase (OD₆₀₀ of 0.07 to 0.1), and the cells were transferred to two 300-ml aliquots of fresh DhA medium at an initial OD₆₀₀ of 0.001. After approximately 45 h of incubation, these cultures reached mid-log phase (OD₆₀₀ values of 0.065 and 0.057), and the cells were harvested.

Harvesting cells. Several aliquots of approximately 10⁹ cells were collected for RNA extraction from each culture (10 ml of succinate-grown cultures or 100 ml of DhA-grown cultures). Immediately after incubation was halted, the cultures were cooled on ice, and an amount of 5% phenol in ethanol equal to 10% of the culture volume was added and mixed by inversion. Cells were harvested by centrifugation at 8,800 \times g at 4°C. A 1.0-ml volume of supernatant from each culture was removed and transferred to a 1.7-ml Eppendorf tube. The remainder of the supernatant was decanted, and the pellets of succinate- or DhA-grown cells were suspended in a small amount of the supernatant (removed in the last step) plus RNAlater (QIAGEN). The cell suspensions were then transferred to 1.7-ml Eppendorf tubes, frozen in liquid nitrogen, and stored at -80°C.

RNA extraction and aminoallyl labeling. RNA extraction and aminoallyl labeling were performed as described in reference 12. Briefly, RNA was extracted by using the RNeasy RNA extraction kit (QIAGEN) according to the manufacturer's instructions. Nucleic acid content was quantified by UV spectroscopy. After RNA extraction, samples were treated with DNase I (Roche) according to the manufacturer's instructions for 30 min at room temperature. The sample was then phenol-chloroform extracted and allowed to air dry for ~5 min. The pellet was then suspended in nuclease-free water and heated at 50°C for 5 to 10 min to dissolve RNA. UV spectroscopy was used to determine RNA quantity and purity. Amino-allyl-labeled cDNA was synthesized by using a protocol adapted from The Institute for Genomic Research (<http://www.tigr.org/tdb/microarray/protocols/TIGR.shtml>). Briefly, 2 μ g of RNA, Random Hexamers (Invitrogen), aminoallyl-dNTP mix (Sigma), and SuperScript II RT (Invitrogen) were combined and incubated for 3 h at 42°C. Purification after enzymatic incorporation was performed by using QiaQuick PCR purification columns (QIAGEN) as described in The Institute for Genomic Research protocol.

Coupling of Cy ester to aminoallyl-labeled cDNA. The amino-allyl-labeled cDNA was subsequently chemically coupled with either Cy3 or Cy5 *N*-hydroxysuccinimidyl ester Cy dye (prepared according to the manufacturer's instructions in dimethyl sulfoxide) and incubated for 1 h in the dark at room temperature. Uncoupled dye was removed by using the QIAGEN QiaQuick PCR purification kit protocol and eluted twice with 30 μ l of the buffer supplied. The quantity of labeled cDNA and the fluorophore incorporation efficiency were determined by using UV-visible spectrophotometry. Cy3/Cy5-labeled cDNA was dried in a speed vacuum and stored at -80°C.

Hybridization. Hybridizations were conducted by using microarray technology developed by Xeotron Technologies (15), and the arrays are have been described

TABLE 2. Growth characteristics of LB400 on four abietane diterpenoids^a

Characteristic	Mean (SE)				
	7-oxo-DhA (<i>n</i> = 4)	DhA (<i>n</i> = 4)	AbA (<i>n</i> = 3)	PaA (<i>n</i> = 3)	Succinate (<i>n</i> = 3)
Lag phase (h)	121 (4)	134 (6)	258 (21)	248 (5)	11.8 (0.12)
Doubling time (h)	23 (4)	17 (1)	37 (2)	19 (1)	2.3 (0.1)
Maximum protein concn (μg/ml of culture)	18.3 (1.2)	25.5 (0.9)	10.9 (1.3)	26.0 (1.1)	ND
Growth yield (g of protein/g of substrate)	0.19 (0.01)	0.28 (0.01)	0.12 (0.01)	0.29 (0.01)	ND

^a Initial inocula were ca. 2×10^6 cells/ml for diterpenoid cultures or ca. 2×10^5 cells/ml for the succinate cultures grown to mid-log phase on succinate. All growth was carried out in K1 mineral salt medium with initial concentrations of 300 μM diterpenoids or 1 g of succinate per liter. *n*, number of replicate cultures.

elsewhere (5, 11). A set of two chips, with probes for 8,450 genes, was used. Briefly, hybridizations were conducted in a Xeotron M-2 microfluidic hybridization station according to the manufacturer's instructions. All buffers were passed through a 0.22-μm-pore-size filter (Corning Costar Corp., Cambridge, MA) prior to hybridization to minimize particulate matter interference with the chips. A total of 200 pmol of labeled cDNA per dye per chip was used for hybridization. Labeled cDNA was suspended in 100 μl of hybridization mix containing 33 μl of 18× SSPE (1× SSPE is 0.18 M NaCl, 10 mM NaH₂PO₄, and 1 mM EDTA; pH 6.6), 25 μl of 100% formamide, and 4 μl of 10% Triton X-100, plus labeled cDNA and nuclease-free water to 100 μl. Samples were heated at 95°C for 3 min, snap cooled on ice for 1 min, and then filtered through 0.22-μm-pore-size filters as described above. Samples were hybridized at 32°C at a flow rate of 300 μl/min for 18 h. Posthybridization was performed to remove nonspecific hybridization by washing with a 6× SSPE solution for 5 min at 32°C at a flow rate of 300 μl/min.

Scanning and data analysis. Microarray scanning and data analysis were conducted as previously reported (11). Briefly, microarrays were scanned by using an Axon 4000B (Axon Instruments) scanner, and data files were extracted by using GenePix 5.0 (Axon Instruments). The data from two genomic subchips were merged and the median signal intensity for both 635 nm (Cy5) and 532 nm (Cy3) were imported into GeneSpring 7.0 (Silicon Genetics) and normalized using Lowess intensity-dependent normalization. A Bayesian moderated *t* test (34) was used to test whether the mean log₂ ratio (DhA/succinate) values of biological replicates were significantly different from zero. In addition, GeneSpring's one-sample Student *t* test algorithm was used to test significant differences. The two analyses agree very closely. Only one gene, BxeC0627, encoding a conserved hypothetical protein, gave opposing results, having a significant log₂ ratio according to the Student *t* test but not the Bayesian *t* test. In general, a gene transcript was considered upregulated when the log₂ ratio was more than 1.0 and the Benjamini Hochberg adjusted *P* value from the Bayesian moderated *t* test was less than 0.05 and was considered downregulated when the log₂ ratio was less than -1.0 and the adjusted *P* value was less than 0.05. Values $M [M = \log_2(\text{Cy5}/\text{Cy3})]$ versus $A [A = \log_2(\sqrt{\text{Cy5} \times \text{Cy3}})]$ were determined for each biological replicate according to the method of Dudoit et al. (14) and plotted to assess normalized data quality (see Fig. S1 in the supplemental material).

Knockout of *ditA1* by gene replacement. LB400 genomic DNA was used as the template in a PCR with primers P1 (5'-ATA GCG CGG GAA CAG TTG CGC CTA CCT GAA G-3') and P4 (5'-TTA GCG CGG GTA TAG ATC AGG TCC TCC GCA-3'), both containing 5' XmaI restriction site extensions (underlined), to amplify a 1,797-bp fragment containing *ditA1*. The resulting amplicon was digested with XmaI and then ligated to the unique dephosphorylated XmaI site of pEX100T, containing the *sacB* counter selectable marker, and used to transform *E. coli* DH5α. Plasmid DNA was then extracted with QIAprep Spin miniprep columns, digested with SphI, and run on a 0.7% agarose gel to identify clones containing inserts with the correct orientation. The successful ligation was designated pDS2. Next, the *XylE-accC1* transcriptional fusion antibiotic cassette of pX1918G was amplified using primer C1 (5'-TAG GCG CGC CGA GAG CAC CGC GAT CAA GGA-3') containing a 5' AscI restriction site extension (underlined) and C2 (5'-CAT GAA TTC CGA ATT CCG ATC CGT CGA GA-3') containing a 5' EcoRI restriction site extension (underlined). The resulting 2.1-kbp amplicon and pDS2 were digested with EcoRI and AscI. Digested pDS2 was run on a 1.0% agarose gel, and a 6,939-bp fragment was extracted from the gel by using a QiaQuick gel extraction kit (QIAGEN). The 2.1-kbp amplicon and 6.9-kbp pDS2 fragment were ligated to generate pDS3, and this was used to transform, by electroporation, mobilization strain *E. coli* S17-1. Homologous recombination of the mutated allele into strain LB400 was accomplished by diparental conjugation using a filter membrane essentially as described previously (10). Briefly, *E. coli* S17-1 containing pDS3 and LB400 was grown overnight on LB with 10 mg of gentamicin/ml and LB without NaCl, respectively. Fresh LB with 10 mg of gentamicin/ml or LB without NaCl was inoculated (10%) with the

respective overnight cultures, and the new cultures were grown until the OD₆₀₀ reached 1 to 1.5. Then, 1 ml of the donor cells (*E. coli* S17-1 containing pDS3) was washed two times with LB and suspended in 1 ml of LB. Next, 100 μl of donor cells and 100 μl of recipient cells were suspended in 0.8% sterile saline and vortexed for 10 s at medium speed. The mating mixture was then transferred to a 5-ml syringe and filtered with a 0.22-μm-pore-size cellulose filter (Millipore GV type) in a reusable filter case. The filter was then removed with forceps and placed with the cells on the upper face on an LB-without-NaCl plate and incubated for ~24 h at 30°C. The filter was then removed with forceps and washed by vortexing in 5 ml of sterile saline, followed by plating on K1 purified 1.5% agar plates supplemented with 1 g of pyruvate per liter plus 10 mg of gentamicin/ml, followed by a two-step selection method as previously described (21). Homologous recombination was confirmed by PCR amplification of a 3,350-kb fragment using primers P1 and P4 at an annealing temperature of 56.3°C identified on an agarose gel. The lack of a 1.7-kbp band and gentamicin resistance further confirmed the desired construct. The 3,350-kbp fragment was also sequenced by using primers P1 and P4, and the resulting sequence was the expected insertion sequence.

RESULTS

LB400 growth on abietane diterpenoids. In growth assays, strain LB400 catabolized the abietane diterpenoids, AbA, DhA, PaA, or 7-oxo-DhA, using each as a sole source of carbon and electrons (Table 2). LB400 failed to grow on the pimarane diterpenoids, isopimaric acid and pimaric acid. Initial lag phases preceding growth on the abietanes were long and variable. The lag phase was shortest on the more soluble, aromatic compounds, 7-oxo-DhA and DhA, and longer on the less-soluble, nonaromatic compounds, AbA and PaA. Although the lag phase on PaA was almost double of that on DhA, the doubling times and yields were similar on the two compounds. 7-oxo-DhA and AbA supported much lower maximum final protein concentrations and growth yields than DhA or PaA. Maximum rates of LB400 growth coincided with maximum rates of substrate removal, and entry into stationary phase coincided with complete removal of the substrates.

Inocula for initial LB400 growth assays on abietane diterpenoids were grown on succinate as described in Materials and Methods. When cells grown on DhA were transferred to fresh medium with DhA, the lag phase was reduced from over 130 h to less than 24 h, and the doubling time was reduced from 17 to approximately 8 h. Further transfers on DhA resulted in minimal change in growth kinetics. A similar effect was observed with serial transfers on AbA, PaA, and 7-oxo-DhA.

Upregulated genes. There were 97 significantly upregulated genes (>2-fold increase in signal intensity, *P* < 0.05) in LB400 grown on DhA compared to on succinate (see Table S1 in the supplemental material). The most striking feature of the DhA transcriptome was a single cluster of 72 genes, from BxeC0578 to BxeC0649, in which 43 genes were significantly upregulated

TABLE 3. Annotation of *dit* cluster and gene expression on DhA

Transcript identification no. ^a	Gene	Product description	COG functional group	Fold upregulation on DhA	Adjusted <i>P</i> value
BxeC0578		Putative transcriptional regulator, TetR/AcrR family	K	1.77	0.031
BxeC0579		Putative ferredoxin reductase	R	6.40	0.158
BxeC0580	<i>ORF2</i>	Putative transporter, MFS family	GEPR	1.52	0.079
BxeC0581	<i>ditF</i>	Conserved hypothetical	R	4.35	1E-03
BxeC0582		Conserved hypothetical	I	2.03	0.019
BxeC0583	<i>ditG</i>	Putative dehydrogenase	QR	5.10	5E-04
BxeC0584		Putative hemerythrin	P	6.78	1E-03
BxeC0585	<i>ditH</i>	Putative hydrolase	Q	6.76	6E-04
BxeC0586	<i>ditA1</i>	Ring-hydroxylating dioxygenase alpha-subunit	PR	2.93	0.025
BxeC0587	<i>ditA2</i>	Ring-hydroxylating dioxygenase beta-subunit	PR	2.93	0.003
BxeC0588		Putative glyoxalase family protein	E	1.68	0.678
BxeC0589		Putative short chain dehydrogenase	QR	1.13	0.823
BxeC0590		Conserved hypothetical	No COG	2.28	0.006
BxeC0591	<i>ditI</i>	Putative short chain dehydrogenase	QR	5.31	0.021
BxeC0592	<i>ditJ</i>	Putative CoA ligase	IQ	7.43	1E-03
BxeC0593	<i>ditK</i>	Putative transcriptional regulator, TetR family	K	1.60	0.045
BxeC0594		Conserved hypothetical	R	2.08	0.033
BxeC0595	<i>ditM</i>	Putative hydrolase	Q	8.20	0.002
BxeC0596	<i>ditN</i>	Putative 3-hydroxyacyl CoA dehydrogenase	I	7.43	1E-03
BxeC0597	<i>ditO</i>	Putative thiolase	I	6.53	0.017
BxeC0598	<i>ditP</i>	Conserved hypothetical	No COG	0.99	0.998
BxeC0599	<i>ditQ</i>	Cytochrome P450	Q	2.43	0.001
BxeC0600		Putative CaiB/BaiF family protein	C	3.95	0.034
BxeC0601		Putative ferredoxin	C	2.48	0.132
BxeC0602		Putative Acyl CoA dehydrogenase	I	3.35	1E-03
BxeC0603		Putative enoyl CoA hydratase	I	3.31	0.001
BxeC0604		Putative acyl CoA dehydrogenase	I	6.70	0.017
BxeC0605		Putative acyl CoA dehydrogenase	I	17.4	0.002
BxeC0606		Conserved hypothetical	No COG	23.4	7E-05
BxeC0607	<i>ditR</i>	Transcriptional regulator, ICLR family	K	1.72	0.052
BxeC0608	<i>ditD</i>	Putative hydrolase	Q	1.23	0.823
BxeC0609		Putative transporter, MFS family	GEPR	3.61	0.002
BxeC0610		Putative short chain dehydrogenase	QR	10.8	0.001
BxeC0611		Hypothetical	No COG	1.13	0.781
BxeC0612		Putative methyl-accepting chemotaxis protein	N	1.43	0.41
BxeC0613		Putative transcriptional regulator, LysR family	K	1.29	0.245
BxeC0614		Putative oxidoreductase	C	2.11	0.079
BxeC0615		Putative transporter, MFS family	E	1.70	0.073
BxeC0616		Putative dehydrogenase	QR	2.98	0.005
BxeC0617		Putative acyl CoA dehydrogenase	I	3.16	0.001
BxeC0618		Putative phosphotransferase	R	3.17	0.001
BxeC0619		Putative short chain dehydrogenase	QR	2.85	0.002
BxeC0620		Putative dehydrogenase	QR	3.76	0.002
BxeC0621		Conserved hypothetical	No COG	6.73	5E-04
BxeC0622		Putative Rieske iron sulfur protein	PR	2.73	0.025
BxeC0623		Conserved hypothetical	PR	3.50	0.001
BxeC0624		Conserved hypothetical	I	1.98	0.107
BxeC0625		Conserved hypothetical	Q	1.78	0.030
BxeC0626		Putative methyl transferase	H	2.28	0.019
BxeC0627		Conserved hypothetical	E	2.57	0.116
BxeC0628		Putative transcriptional regulator, TetR/AcrR family	K	1.10	0.823
BxeC0629		Conserved hypothetical	No COG	1.04	0.943
BxeC0630		Conserved hypothetical	No COG	0.99	0.987
BxeC0631	<i>ditU</i>	Cytochrome P450	Q	1.11	0.834
BxeC0632		Putative AraC type transcriptional regulator	K	1.24	0.823
BxeC0633		Conserved hypothetical	No COG	1.34	0.201
BxeC0634		Conserved hypothetical	No COG	1.46	0.387
BxeC0635		Putative dehydrogenase	QR	1.23	0.823
BxeC0636		Putative transcriptional regulator, TetR/AcrR Family	K	1.07	0.693
BxeC0637		Conserved hypothetical	Q	1.16	0.771
BxeC0638	<i>ditA3</i>	Ferredoxin	C	7.38	9E-04
BxeC0639	<i>ditB</i>	Putative dehydrogenase	QR	5.10	0.001
BxeC0640	<i>ditC</i>	Aromatic ring cleavage dioxygenase	No COG	5.60	0.003
BxeC0641		Conserved hypothetical	R(I)	3.15	0.002
BxeC0642		Putative dehydrogenase	QR	21.2	7E-05
BxeC0643		Putative enoyl CoA hydratase/isomerase	I	18.4	0.014
BxeC0644		Conserved hypothetical	E	9.15	0.019
BxeC0645		Putative transporter, RND superfamily	R	7.34	1E-03
BxeC0646		Conserved hypothetical	No COG	7.88	9E-04
BxeC0647		Conserved hypothetical	No COG	5.54	0.019
BxeC0648		Conserved hypothetical	No COG	6.38	1E-03
BxeC0649		Putative transcriptional regulator, TetR/AcrR family	K	1.12	0.823

^a Putative cotranscripts are shown in boxes.

(Table 3 and Fig. 1). The cluster is located on the LB400 megaplasmid and, based on patterns of expression, gene orientation, and gene proximity, encompasses 10 putative mRNA transcripts that were upregulated. The cluster contains all of

the 22 LB400 genes previously identified as homologs of BKME-9 *dit* genes (33), as well as a number of additional genes likely involved in catabolism. The cluster contains all of the 17 upregulated genes from the orthologous group of pro-

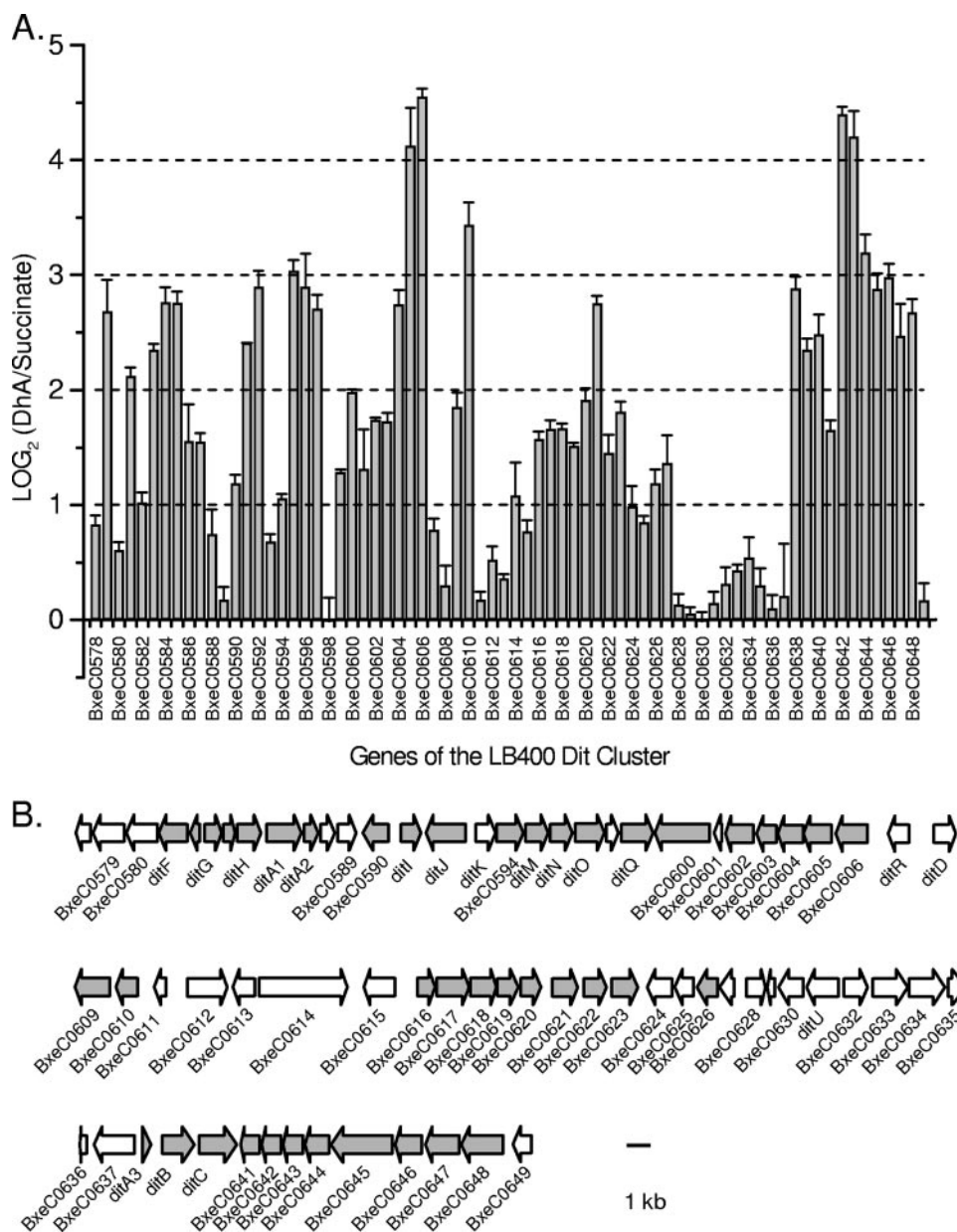


FIG. 1. (A) Relative signal intensities for genes of the LB400 *dit* cluster during growth on DhA versus on succinate. Error bars indicate the standard error. (B) Physical map of the LB400 *dit* cluster. The three rows of arrows represent one contiguous cluster of genes, showing gene size and orientation. Shaded arrows represent genes significantly upregulated on DhA.

teins (COG) group Q, which comprises genes encoding metabolite biosynthesis, transport, and catabolism. This cluster also contains 10 of 16 upregulated genes from COG group I, which comprises lipid metabolism and is the group with the greatest number of genes upregulated on DhA. Many of these genes encode enzymes that catalyze beta-oxidation type reactions, which are expected to be important in the later stages of abietane degradation, after cleavage of the ring structures to branched, substituted alkanes. Because of the putative role of the above gene cluster in diterpenoid catabolism, we refer to it as the LB400 *dit* cluster.

There were additional noteworthy groups of contiguous and functionally related genes upregulated on DhA and located out-

side of the *dit* cluster. One such group (BxeB2300, BxeB2300, and BxeB2302) encodes citrate/aconitate metabolism, which may reflect modulation of central metabolism to accommodate abietane diterpenoid catabolism. Three upregulated genes, including two linked genes (BxeB2301, BxeB2302, and BxeB1203) encode the necessary steps for catabolism of propionyl-CoA, which commonly results from alkane degradation. Two upregulated groups of genes putatively encode sulfate uptake (BxeA2467, BxeA2469, and BxeA2470) and sulfate metabolism (BxeA3659, BxeA3660, BxeA3663, BxeA3664, and BxeA3671). However, the relationship between sulfate and abietane diterpenoid metabolism is unclear. Another upregulated group (BxeB2702 to BxeB2709) is conserved in *Bradyrhizobium japonicum*, with deduced amino acid

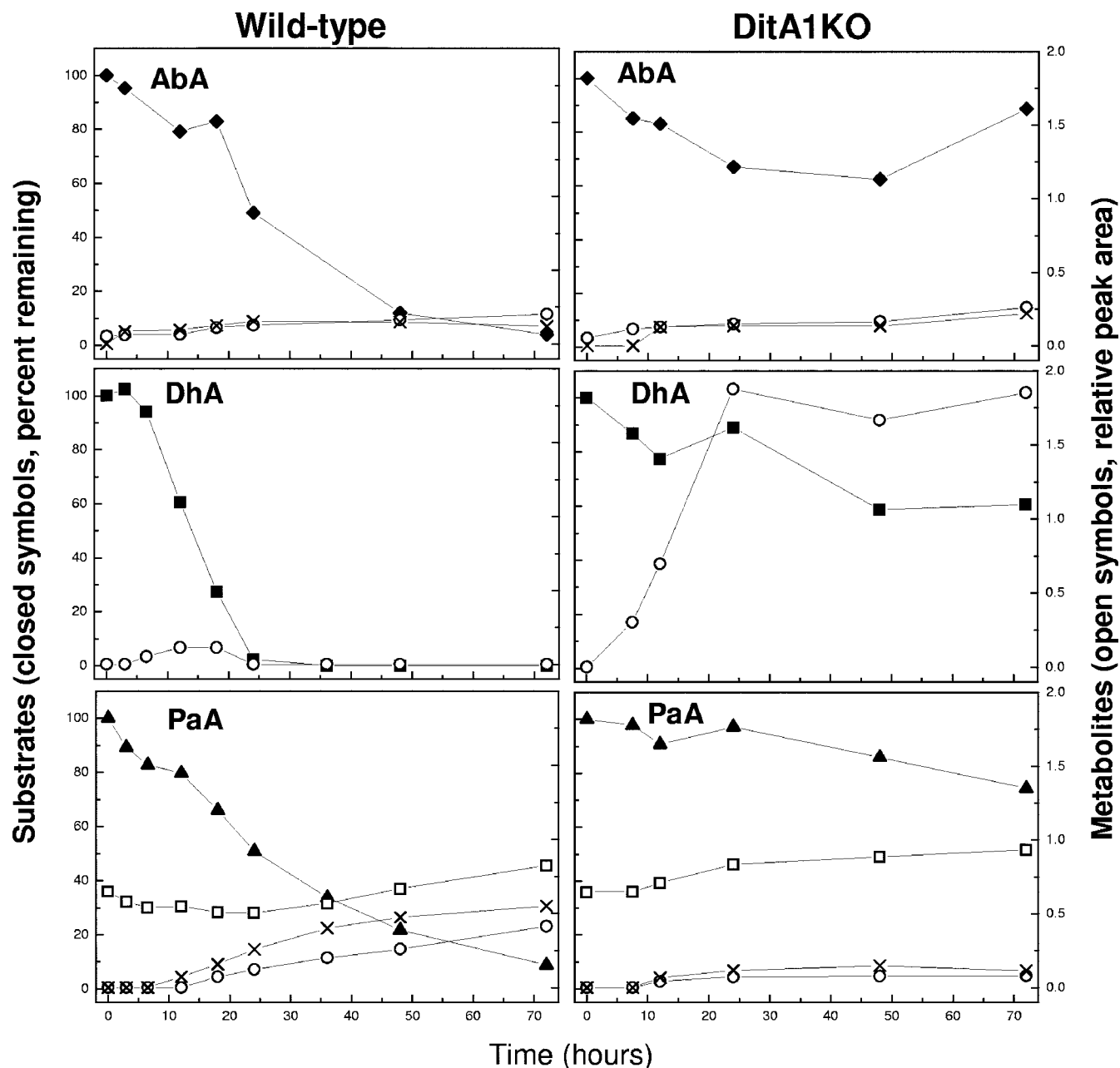


FIG. 2. Incubation of cell suspensions of wild-type and *DitA1KO* with AbA, DhA, and PaA. Closed symbols indicate values corresponding to the left y axis, and open or stick symbols indicate values corresponding to the right y axis. Symbols: \blacklozenge , AbA; \blacksquare and \square , DhA; \blacktriangle , PaA; \circ , 7-oxo-DhA; \times , 7-oxo-PaA. The relative peak area is the area of the metabolite peak divided by that of the internal standard. The data are for a single experiment. A replicate experiment with cells from an independent culture exhibited the same patterns of substrate removal and metabolite appearance. However, the independent experiments were slightly out of phase, so the data were not averaged.

identity of 48 to 56% and identical gene order. This group encodes an ABC transport system and an enzyme system most similar to opine oxidase. Opines are plant produced amino acids resulting from infection of *Agrobacterium tumefaciens* in plant rhizospheres, which are cleaved by opine oxidase to yield pyruvate or 2-ketoglutarate plus L-arginine (39).

Downregulated genes. There were 39 significantly downregulated genes (>2 -fold decrease in signal intensity, $P < 0.05$) on DhA compared to on succinate (see Table S2 in the sup-

plemental material). None of the downregulated genes are in the *dit* cluster. Four signal transduction (COG T) proteins are encoded by genes that are downregulated, compared to no upregulated genes in this group. Two COG T genes, BxeA4195 and BxeA4196, are adjacent and immediately downstream of a downregulated gene encoding a putative C4-dicarboxylate transport protein BxeA4197 (COG C, energy production and conversion) possibly involved in succinate transport. Other downregulated COG C genes include BxeB1810, encoding a

putative oxygen-dependent terminal cytochrome *bd* oxidase subunit 1; BxeA0283, encoding a putative malate dehydrogenase; and BxeA3313, encoding a putative cytochrome *c*. Overall, the downregulated COG C genes might indicate a slowing of central metabolism to accommodate slower growth on DhA than on succinate. In addition, a group of four downregulated genes, BxeA0132, BxeA0141, BxeA0143, and BxeA0157, putatively encode flagellar synthesis proteins (COG N).

DitA1KO. To confirm that the LB400 *dit* cluster contains genes required for abietane degradation, we generated a knockout of *ditA1*, hypothesized to be essential for abietane diterpenoid degradation. The resulting strain, DitA1KO, lacks the alpha-subunit (catalytic subunit) of a ring-hydroxylating dioxygenase system, DitA. After 400 h of incubation, DitA1KO failed to grow on AbA, DhA, PaA, or 7-oxo-DhA as sole organic substrates, thus confirming the essentiality of DitA for catabolism of these compounds.

LB400 and DitA1KO cell suspensions. Cell suspensions of wild-type LB400 removed AbA, DhA, PaA, or 7-oxo-DhA completely, whereas DitA1KO only slightly reduced concentrations of these substrates (Fig. 2). As previously reported for other strains (23), boiling the cells prior to incubation nearly abolished the removal of abietane diterpenoids; however, some initial removal (<20%) was detected. In these cases, no metabolites were formed. Therefore, removal was likely the result of sorption of diterpenoids to the cells or the culture tubes rather than metabolism.

7-Oxo-DhA was detected in both wild-type and DitA1KO cell suspensions (Fig. 2). With AbA, DhA, or PaA, wild-type LB400 transiently accumulated small amounts of 7-oxo-DhA, which were completely removed within 144 h in all cases (data not shown). DitA1KO also accumulated 7-oxo-DhA, which it did not remove, even after 144 h of incubation. DitA1KO accumulated much more 7-oxo-DhA from DhA than from AbA or PaA. A second metabolite accumulated in both wild-type and DitA1KO cell suspensions incubated with AbA and PaA but not in those incubated with DhA. This metabolite could not be identified using the National Institute of Standards and Technology library, but its mass spectrum strongly supports its identification as 7-oxo-PaA, whose spectrum is not in the library. Five of the main peaks in the mass spectrum support this identification: *m/z* 330 (molecular ion, M), *m/z* 315 (M - CH₃), *m/z* 271 (M - COOCH₃), *m/z* 270 (M - HCOOCH₃), and *m/z* 255 (M - CH₃ - HCOOCH₃). This fragmentation pattern corresponds to that reported for 7-oxo-DhA (37), except all of the major ions are 2 mass units greater than the corresponding ones from 7-oxo-DhA (Fig. 3).

In cell suspensions of both wild-type LB400 and DitA1KO with PaA, DhA was initially present as a contaminant of the PaA substrate and was stable or gradually increased to a maximum concentration at 72 h (Fig. 2). After 96 h, all accumulated DhA was removed by the wild-type, but DhA remained at a constant level in cell suspensions of DitA1KO for at least 144 h (not shown). The DhA concentration did not increase during incubation of boiled cell controls for 144 h, indicating any transformation of PaA to DhA was enzymatic. In cell suspensions with 7-oxo-DhA (data not shown), the substrate was removed within 24 h by the wild-type strain and not removed by ditA1KO strain.

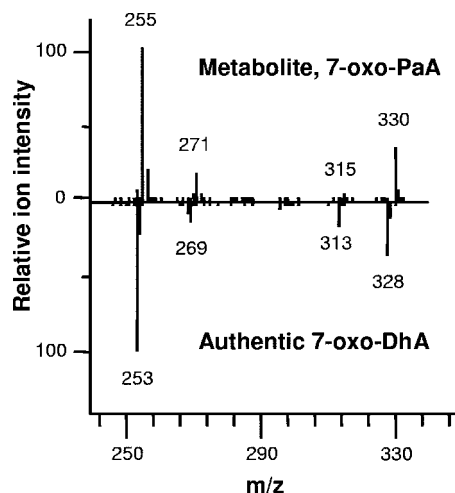


FIG. 3. Identification of 7-oxo-PaA metabolite. Head-to-tail mass spectra of 7-oxo-DhA authentic standard versus metabolite detected in cell suspensions are shown.

DISCUSSION

Competitiveness of LB400. This study demonstrates that LB400 is able to catabolize abietane diterpenoids as can several other bacteria (reviewed in references 24 and 26). However, in our initial growth tests, LB400 exhibited a much longer lag phase and lower growth rate (Table 2) than other characterized abietane-degrading bacteria (23, 33). The reason for this lag phase is unclear, but the time seems too long to be solely due to genetic induction. Most abietane degraders were obtained from sources such as forest soil, pulp and paper mill effluent, or bioreactors via selective enrichment on abietanes, which would have selected organisms growing relatively fast on abietanes under the enrichment conditions. In contrast, LB400 was not obtained via such enrichment and is unlikely to be competitive under such enrichment conditions. However, growth yields of LB400 on DhA were similar to those of abietane degraders such as *Sphingomonas* sp. strain DhA-33, *Zooletta* sp. strain DhA-35, and *Pseudomonas abietaniphila* BKME-9 (24, 33). Further, after multiple passages on abietanes, LB400 cultures attained shorter lag phases and higher growth rates typical of other abietane degraders. Under conditions where abietanes are continuously available, such as wastewater treatment systems or perhaps some plant-associated environments, LB400 would grow at similar rates as other abietane degraders and would potentially be competitive with those organisms.

LB400 *dit* cluster. From the sum of the evidence, it is clear that many of the 72 genes in the LB400 *dit* cluster are directly responsible for DhA catabolism, and it seems likely that the cluster encodes most of the proteins necessary for the degradation of abietanes to central metabolites. The LB400 *dit* cluster contains homologs of all but one gene previously associated with abietane catabolism. These comprise 22 genes of the *Pseudomonas abietaniphila* BKME-9 *dit* cluster (33), seven of which are also in the *Pseudomonas diterpeniphila* A19-6a *tdt* cluster (25). The sole outstanding gene not found in LB400 is *ditE* from BKME-9, encoding a putative permease of the major facilitator superfamily. The homologous genes from the three strains have very high similarity, at least 49% identity of tran-

scribed proteins. From our fragmentary knowledge of the BKME-9 *dit* cluster and A19-6a *tdt* cluster, it further appears that gene order is also partly conserved among the three organisms.

This and previous studies provide additional evidence through knockout analysis for the roles in abietane degradation of several of the LB400 *dit* cluster genes, which were upregulated on DhA. Our analysis of the Dita1KO strain confirms the essentiality of *ditA1*, encoding the alpha-subunit of a ring-hydroxylating dioxygenase, for the catabolism of all four abietane diterpenoids tested, which is consistent with a previous findings for *ditA1* in BKME-9 (21). Through previous gene knockout analysis, very similar orthologs of six additional genes of the LB400 *dit* cluster were shown to be required for abietane diterpenoid metabolism. These orthologs include *ditA3*, *ditC*, *ditF*, *ditH*, and *ditI* in BKME-9 (20), as well as *tdtL* (orthologous to *ditJ*) in A19-6a (25).

The present study substantially increases the number of genes and proteins associated with diterpenoid degradation. When LB400 grew on DhA, a majority of the *dit* cluster genes, at least 43, plus others in several smaller clusters, were upregulated. Of the upregulated LB400 *dit* cluster genes, 22 were not previously associated with abietane degradation. The latter genes encode proteins responsible for beta-oxidation, transport, and general catabolism, which are functions logically involved in abietane catabolism. Genes in the cluster not upregulated on DhA may have other roles, possibly including catabolism of other abietanes. We have not excluded the possibility that some genes in the *dit* cluster are unrelated to abietane catabolism.

A possible catabolic transposon. Several observations indicate that the *dit* cluster is mobile and widely distributed among proteobacterial genomes and suggest that the LB400 *dit* cluster is a large catabolic transposon. Catabolic transposons have a wide variety of sizes and have been reported to be as large as 90 kb in length (35). The genomes of *Burkholderia* spp., including LB400, are rich in insertion sequences (19). The LB400 megaplasmid contains several transposases, including several flanking the *dit* cluster (BxeC0485 to BxeC0490, BxeC0519, and BxeC0670 to BxeC0672), whereas no transposase genes were identified within the *dit* cluster. Further, the GC content of the LB400 *dit* cluster is 64.9% versus 61.7% for the total megaplasmid and 62.6% for the total genome. Chain et al. (5) reported the presence of the *dit* cluster of genes in two additional *B. xenovorans* strains, LMG21720 and LMG16224, which are both able to grown on AbA or DhA. (T. Tsoi, unpublished data). Interestingly, one of these strains did not contain a megaplasmid, implying that the *dit* cluster was encoded on chromosome 1 or 2 of that strain. As mentioned above, at least part of the LB400 *dit* cluster is conserved in *P. abietaniphila* BKME-9 (33) and *P. diterpeniphila* A19-6a (25). Further, a cluster of genes with high sequence identity and similar gene arrangement to that of the LB400 *dit* cluster was identified in the recently sequenced genome of *P. aeruginosa* 2192 (*Pseudomonas aeruginosa* 2192 Sequencing Project, Broad Institute of Harvard and MIT [http://www.broad.mit.edu]). It is not yet known whether this latter strain can grow on abietane diterpenoids. The genera *Burkholderia*, within the class *Betaproteobacteria*, and *Pseudomonas*, within the class *Gammaproteobacteria*, are well-separated phylogenetic groups.

Uptake of abietanes. The LB400 *dit* cluster encodes a number of proteins with potential roles in abietane uptake. These proteins include four permeases, three members of the major facilitator superfamily (MFS) and one member of the resistance nodulation (RND) cell division superfamily. Genes BxeC0609 and BxeC0645 encoding two of these permeases were significantly upregulated during growth on DhA (Fig. 1 and Table 3). The RND permease, encoded by BxeC0645, seems particularly likely to play a role in abietane uptake. This deduced protein contains 835 amino acids, with 12 predicted transmembrane subunits (TMS) and two large hydrophilic extracytoplasmic domains, between TMS 1 and 2 and between TMS 7 and 8. Members of this family are found among diverse phyla and participate in a wide range of transport activities (36). Analysis of the protein encoded by BxeC0645 using the Prosite database (http://www.expasy.org/prosite/) identified a sterol-sensing domain (residues 278 to 400) comprised of five predicted membrane-spanning helices with short intervening loops. A similar sterol-sensing domain from a purified hamster protein involved in lipid homeostasis was shown to directly bind cholesterol (29). Another member of the RND family, NPC1L1, also containing a sterol-sensing domain, was found to facilitate intestinal cholesterol absorption in mice (2). Given the structural similarity between steroids and abietanes, these findings suggest that BxeC0645 may encode a diterpenoid transport protein responsible for uptake of DhA, a possibility supported by the location of BxeC0645 in the *dit* cluster and its relatively high level of upregulation on DhA. Genes BxeC0646 and BxeC0648 appear to be cotranscribed with BxeC0645 and encode conserved hypothetical proteins containing signal peptides, which may also function in a membrane-associated transport system.

Abietane metabolism. Cell suspension assays of LB400 and Dita1KO show that the abietane diterpenoid catabolic pathway of LB400 is similar to the convergent pathway proposed for BKME-9 (33) and differs from that proposed for *Arthrobacter* sp. and *Flavobacterium resinovorum* (as reviewed in reference 18). The former involves a 7-oxo-DhA intermediate (Fig. 4), while the latter proceeds through a 3-oxo-DhA intermediate. Previously, we showed evidence that BKME-9 hydroxylates DhA, AbA, and PaA at C7, forming 7-hydroxy-DhA. This metabolite was identified in the supernatant of *Alcaligenes eutrophus* growing on DhA (3). Oxidation of the C7 alcohol to a C7 ketone by an as-yet-unidentified dehydrogenase would form 7-oxo-DhA. 7-oxo-DhA was shown to be the substrate of the Dita_{BKME-9} ring-hydroxylating dioxygenase, which, with a putative *cis*-dihydrodiol dehydrogenase, forms 11,12-dyhydroxy-7-oxo-DhA (21). Accordingly, 7-oxo-DhA accumulated in BKME-9 *ditA1* knockout mutants metabolizing DhA (21). In agreement with these reports, we observed here that wild-type LB400 accumulated small amounts of 7-oxo-DhA during metabolism of DhA and that Dita1KO accumulated much larger amounts of 7-oxo-DhA from DhA (Fig. 2).

Formation of 7-oxo-DhA during AbA and PaA metabolism by LB400 appears to occur through a 7-oxo-PaA intermediate (Fig. 4). Supporting that pathway, 7-oxo-PaA, was detected in both wild-type and Dita1KO cell suspensions metabolizing AbA or PaA but not those metabolizing DhA. Although it was not identified, the same metabolite was previously detected in cell suspensions of a BKME-9 *ditA1* mutant incubated with

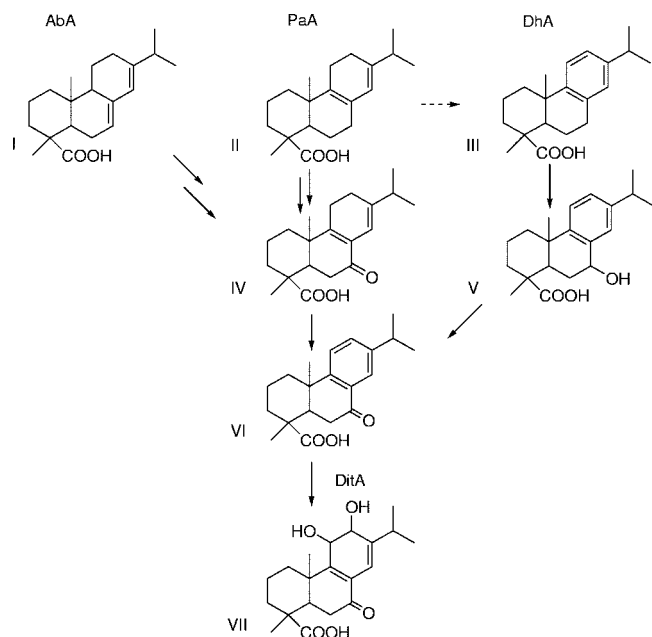


FIG. 4. Proposed convergent pathway for abietane diterpenoid degradation by LB400. I, abietic acid; II, palustric acid; III, dehydroabietic acid; IV, 7-oxo-palustric acid; V, 7-hydroxy-dehydroabietic acid; VI, 7-oxo-dehydroabietic acid; VII, 7-oxo-11,12-dihydroxy-8,13-abietadiene acid.

PaA (20), suggesting that this pathway is common to both BKME-9 and LB400. Previously, we demonstrated the partial transformation of PaA to DhA by BKME-9, involving aromatization of the C ring (33). Possible increases of DhA in both LB400 wild-type and Dita1KO cell suspensions metabolizing PaA (Fig. 2) are consistent with LB400 also catalyzing this transformation, but the evidence is not as clear as it was for BKME-9. This transformation may comprise a second route for PaA degradation, with relative fluxes of PaA through the two pathways being uncertain.

Oxygenase electron transport systems. Analysis of the LB400 *dit* cluster sheds light on the subunit composition of oxygenase systems involved in abietane catabolism. Frequently, genes encoding the components of multicomponent oxygenases are located in a single operon, as for the LB400 *bphAEFG* genes, encoding biphenyl dioxygenase (12). In contrast, the LB400 *dit* cluster encodes three oxygenase systems—DitA, DitQ, and DitU—lacking obvious electron transport systems. Such electron transport systems are comprised of a ferredoxin plus a ferredoxin reductase and are essential for activity of the catalytic subunits. The catalytic subunit genes, *ditA1A2* and *ditQ*, were upregulated on DhA, whereas *ditU* was not (Table 3 and Fig. 1). Within the LB400 *dit* cluster, but not directly linked to the catalytic subunit genes, are genes encoding two ferredoxins (BxeC0601 and *ditA3*) and a putative ferredoxin reductase (BxeC0579). These three genes were all upregulated on DhA, and no other paralogous genes outside of the *dit* cluster were upregulated. Thus, BxeC0579 and one or both of the ferredoxin genes likely encode electron transport components of oxygenases involved in DhA degradation.

Previous studies of Dita_{BKME-9} strongly suggest that *ditA3* encodes a ferredoxin that functions with Dita_{LB400}. Dita₃_{LB400} is

56.7% identical to the 3Fe-4S ferredoxin, Dita₃_{BKME-9} (9), whereas the ferredoxin encoded by BxeC0601 is only 8.4% identical to Dita₃_{BKME-9} and is a 2Fe-2S ferredoxin. In BKME-9, knocking out *ditA3* abolished the ability to grow on abietanes (20). Further, a functional 7-oxo-DhA dioxygenase system was demonstrated by expressing Dita1A2A3_{BKME-9} in *E. coli* (21). The Dita₃_{BKME-9} ferredoxin was essential to this system, while the *E. coli* host provided a surrogate ferredoxin reductase. The possibility that the ferredoxin encoded by BxeC0601 can also function with Dita_{LB400} has not been ruled out, and it remains unclear which ferredoxin(s) function with the P450 monooxygenases DitQ and DitU.

The present study complements previous fragmentary evidence for a ferredoxin reductase for Dita_{BKME-9} and suggests that the putative ferredoxin reductase encoded by BxeC0579 functions in one or more of the *dit* oxygenase systems. This gene was previously annotated as encoding a putative pyridine nucleotide-disulfide oxidoreductase, but several lines of evidence support changing that annotation. This protein shares 51% amino acid sequence identity with ThcD from *Rhodococcus erythropolis* (27) and 50% amino acid sequence identity with EthA from *Rhodococcus ruber* (6), which serve as ferredoxin reductases in P450 systems involved in the degradation of *S*-ethyl dipropylcarbamothiolate and ethyl *tert*-butyl ether, respectively. A fragment of a ferredoxin reductase gene, essential for growth of BKME-9 on DhA, was identified through transposon mutagenesis (22). Sequencing the region flanking a transposon insertion, which abolished growth on DhA, revealed a gene fragment encoding a 119-amino-acid sequence 65% identical to residues 261 to 380 of the product of BxeC0579. Based on this sequence analysis, the genomic context of the gene, and the fact that no other ferredoxin reductase gene was upregulated on DhA, we postulate that BxeC0579 encodes a ferredoxin reductase functioning in Dita_{LB400} and, possibly, the DitQ monooxygenase. A common electron transport system, shared by both monooxygenase and dioxygenase systems, was previously demonstrated in the catabolic pathway for naphthalene in *Ralstonia* sp. strain U2 (40).

ACKNOWLEDGMENTS

We thank John Parnell and Edmilson Gonçalves for assistance with preparation of labeled cDNA, Hirofumi Hara and Vincent Deneff for assistance with analysis of transcriptomic data, and Gordon Stewart for assistance with MS analysis.

This research was supported by a Discovery Grant from the Natural Sciences and Engineering Council of Canada.

REFERENCES

1. Ali, M., and T. R. Sreekrishnan. 2001. Aquatic toxicity from pulp and paper mill effluents: a review. *Adv. Environ. Res.* 5:175–196.
2. Altmann, S. W., H. R. Davis, Jr., L. J. Zhu, X. Yao, L. M. Hoos, G. Tetzloff, S. P. N. Iyer, M. Maguire, and A. Golovko. 2004. Niemann-Pick C1-like 1 protein is critical for intestinal cholesterol absorption. *Science* 303:1201–1204.
3. Biellmann, J. F., G. Branlant, M. Gero-Robert, and M. Poiret. 1973. Dégradation bactérienne de l'acide dehydroabietique par un *Pseudomonas* et une *Alcaligenes*. *Tetrahedron* 29:1237–1241.
4. Byun-McKay, A., K. A. Godard, M. Toudefallah, D. M. Martin, R. Alfaro, J. King, J. Bohlmann, and A. L. Plant. 2006. Wound-induced terpene synthase gene expression in Sitka spruce that exhibit resistance or susceptibility to attack by the white pine weevil. *Plant Physiol.* 140:1009–1021.
5. Chain, P. S., V. J. Deneff, K. T. Konstantinidis, L. M. Vergez, L. Agulló, V. L. Reyes, L. Hauser, M. Córdova, L. Gómez, M. González, M. Land, V. Lao, F. Larimer, J. J. LiPuma, E. Mahenthalingam, S. A. Malfatti, C. J. Marx, J. J. Parnell, A. Ramette, P. Richardson, M. Seeger, D. Smith, T. Spilker, T. V.

- Tsoi, L. E. Ulrich, I. B. Zhulin, and J. M. Tiedje. 2006. *Burkholderia xenovorans* LB400 harbors a multi-replicon, 9.7-Mbp genome shaped for versatility. *Proc. Natl. Acad. Sci. USA* **103**:15280–15287.
6. Chauvaux, S., F. Chevalier, C. Le Dantec, F. Fayolle, I. Miras, F. Kunst, and P. Beguin. 2001. Cloning of a genetically unstable cytochrome P-450 gene cluster involved in degradation of the pollutant ethyl *tert*-butyl ether by *Rhodococcus ruber*. *J. Bacteriol.* **183**:6551–6557.
 7. Chen, W.-M., L. Moulin, C. Bontemps, P. Vandamme, G. Bena, and C. Boivin-Masson. 2003. Legume symbiotic nitrogen fixation by beta-proteobacteria is widespread in nature. *J. Bacteriol.* **185**:7266–7272.
 8. Coenye, T., and P. Vandamme. 2003. Diversity and significance of *Burkholderia* species occupying diverse ecological niches. *Environ. Microbiol.* **5**:719–729.
 9. Couture, M. M.-J., V. J. J. Martin, W. W. Mohn, and L. E. Eltis. 2006. Characterization of DitaA3, the [Fe3S4] ferredoxin of an aromatic ring-hydroxylating dioxygenase from a diterpenoid-degrading microorganism. *Biochim. Biophys. Acta* **1764**:1462–1469.
 10. de Lorenzo, V., and K. N. Timmis. 1994. Analysis and construction of stable phenotypes in gram-negative bacteria with Tn5- and Tn10-derived minitransposons. *Methods Enzymol.* **235**:386–405.
 11. Denef, V. J., J. A. Klappenbach, M. A. Patrauchan, C. Florizone, J. L. M. Rodrigues, T. V. Tsoi, W. Verstraete, L. D. Eltis, and J. M. Tiedje. 2006. Genetic and genomic insights into the role of benzoate-catabolic pathway redundancy in *Burkholderia xenovorans* LB400. *Appl. Environ. Microbiol.* **72**:585–595.
 12. Denef, V. J., J. Park, T. V. Tsoi, J.-M. Rouillard, H. Zhang, J. A. Wibbenmeyer, W. Verstraete, E. Gulari, S. A. Hashsham, and J. M. Tiedje. 2004. Biphenyl and benzoate metabolism in a genomic context: outlining genome-wide metabolic networks in *Burkholderia xenovorans* LB400. *Appl. Environ. Microbiol.* **70**:4961–4970.
 13. Denef, V. J., M. A. Patrauchan, C. Florizone, J. Park, T. V. Tsoi, W. Verstraete, J. M. Tiedje, and L. D. Eltis. 2005. Growth substrate- and phase-specific expression of biphenyl, benzoate, and C1 metabolic pathways in *Burkholderia xenovorans* LB400. *J. Bacteriol.* **187**:7996–8005.
 14. Dudoit, S., Y. H. Yang, J. C. Callow, and T. P. Speed. 2002. Statistical methods for identifying differentially expressed genes in replicated cDNA microarray experiments. *Statistica Sinica* **12**:111–139.
 15. Gao, X., E. LeProust, H. Zhang, O. Srivannavit, E. Gulari, P. Yu, C. Nishiguchi, Q. Xiang, and X. Zhou. 2001. A flexible light-directed DNA chip synthesis gated by deprotection using solution photogenerated acids. *Nucleic Acids Res.* **29**:4744–4750.
 16. Goris, J., P. De Vos, J. Caballero-Mellado, J. Park, E. Falsen, J. F. Quensen III, J. M. Tiedje, and P. Vandamme. 2004. Classification of the biphenyl- and polychlorinated biphenyl-degrading strain LB400^T and relatives as *Burkholderia xenovorans* sp. nov. *Int. J. Syst. Evol. Microbiol.* **54**:1677–1681.
 17. Kamaya, Y., N. Tokita, and K. Suzuki. 2005. Effects of dehydroabietic acid and abietic acid on survival, reproduction, and growth of the crustacean *Daphnia magna*. *Ecotoxicol. Environ. Saf.* **61**:83–88.
 18. Kieslich, K. 1976. Microbial transformations of non-steroid cyclic compounds. John Wiley & Sons, Ltd., Chichester, England.
 19. Lessie, T. G., W. Hendrickson, B. D. Manning, and R. Devereux. 1996. Genomic complexity and plasticity of *Burkholderia cepacia*. *FEMS Microbiol. Lett.* **144**:117–128.
 20. Martin, V. J., and W. W. Mohn. 2000. Genetic investigation of the catabolic pathway for degradation of abietane diterpenoids by *Pseudomonas abietaniphila* BKME-9. *J. Bacteriol.* **182**:3784–3793.
 21. Martin, V. J., and W. W. Mohn. 1999. A novel aromatic-ring-hydroxylating dioxygenase from the diterpenoid-degrading bacterium *Pseudomonas abietaniphila* BKME-9. *J. Bacteriol.* **181**:2675–2682.
 22. Martin, V. J. J. 1999. Molecular genetic investigation of the abietane diterpenoid degradation pathway of *Pseudomonas abietaniphila* BKME-9. Ph.D. thesis. University of British Columbia, Vancouver, British Columbia, Canada.
 23. Mohn, W. W. 1995. Bacteria obtained from a sequencing batch reactor that are capable of growth on dehydroabietic acid. *Appl. Environ. Microbiol.* **61**:2145–2150.
 24. Mohn, W. W., A. E. Wilson, P. Bicho, and E. R. Moore. 1999. Physiological and phylogenetic diversity of bacteria growing on resin acids. *Syst. Appl. Microbiol.* **22**:68–78.
 25. Morgan, C. A., and R. C. Wyndham. 2002. Characterization of *tdt* genes for the degradation of tricyclic diterpenes by *Pseudomonas diterpeniphila* A19-6a. *Can. J. Microbiol.* **48**:49–59.
 26. Morgan, C. A., and R. C. Wyndham. 1996. Isolation and characterization of resin acid degrading bacteria found in effluent from a bleached kraft pulp mill. *Can. J. Microbiol.* **42**:423–430.
 27. Nagy, L., G. Schoofs, F. Compennolle, P. Proost, J. Vanderleyden, and R. de Mot. 1995. Degradation of the thiocarbamate herbicide EPTC (*S*-ethyl dipropylcarbamothioate) and biosafening by *Rhodococcus* sp. strain NI86/21 involve an inducible cytochrome P-450 system and aldehyde dehydrogenase. *J. Bacteriol.* **177**:676–687.
 28. Partida-Martinez, L. P., and C. Hertweck. 2005. Pathogenic fungus harbours endosymbiotic bacteria for toxin production. *Nature* **437**:884–888.
 29. Radhakrishnan, A., L. P. Sun, H. J. Kwon, M. S. Brown, and J. L. Goldstein. 2004. Direct binding of cholesterol to the purified membrane region of SCAP: mechanism for a sterol-sensing domain. *Mol. Cell* **15**:259–268.
 30. Sanford, J. P. 1995. *Pseudomonas* species (including melioidosis and glanders), p. 2003–2009. In G. L. Mandell, J. E. Bennett, and R. Dolin (ed.), *Principles and practice of infectious diseases*, 4th ed. Churchill Livingstone, New York, NY.
 31. Schweizer, H. P., and T. T. Hoang. 1995. An improved system for gene replacement and *xylE* fusion analysis in *Pseudomonas aeruginosa*. *Gene* **158**:15–22.
 32. Simons, R., U. Priefer, and A. Puhler. 1983. A broad host range mobilization system for in vivo genetic engineering: transposon mutagenesis in gram-negative bacteria. *Bio/Technology* **1**:784–790.
 33. Smith, D. J., V. J. Martin, and W. W. Mohn. 2004. A cytochrome P450 involved in the metabolism of abietane diterpenoids by *Pseudomonas abietaniphila* BKME-9. *J. Bacteriol.* **186**:3631–3639.
 34. Smyth, G. K. 2004. Linear models and empirical Bayes methods for assessing differential expression in microarray experiments. *Stat. Appl. Genet. Mol. Biol.* **3**:Article 3.
 35. Tan, H.-M. 1999. Bacterial catabolic transposons. *Appl. Microbiol. Biotechnol.* **51**:1–12.
 36. Tseng, T. T., K. S. Gratwick, J. Kollman, D. Park, D. H. Nies, A. Goffeau, and M. H. Saier, Jr. 1999. The RND permease superfamily: an ancient, ubiquitous and diverse family that includes human disease and development proteins. *J. Mol. Microbiol. Biotechnol.* **1**:107–125.
 37. van den Berg, K. J., J. J. Boon, I. Patorova, and F. M. Spetter. 2000. Mass spectrometric methodology for the analysis of highly oxidized diterpenoid acids in Old Master paintings. *J. Mass Spectrom.* **35**:512–533.
 38. White, N. J. 2003. Melioidosis. *Lancet* **361**:1715–1722.
 39. Zanker, H., G. Lurz, U. Langridge, P. Langridge, D. Kreuzsch, and J. Schroder. 1994. Octopine and nopaline oxidases from Ti plasmids of *Agrobacterium tumefaciens*: molecular analysis, relationship, and functional characterization. *J. Bacteriol.* **176**:4511–4517.
 40. Zhou, N.-Y., J. Al-Dulayymi, M. S. Baird, and P. A. Williams. 2002. Salicylate 5-hydroxylase from *Ralstonia* sp. strain U2: a monooxygenase with close relationships to and shared electron transport proteins with naphthalene dioxygenase. *J. Bacteriol.* **184**:1547–1555.